THE JOURNAL OF BIOLOGICAL CHEMISTRY VOL. 287, NO. 50, pp. 42031–42041, December 7, 2012

The Organization of a CSN5-containing Subcomplex of the COP9 Signalosome*[S]

Received for publication, June 4, 2012, and in revised form, September 19, 2012 Published, JBC Papers in Press, October 18, 2012, DOI 10.1074/jbc.M112.387977

Giri Gowda Kotiguda[‡§1], Dahlia Weinberg[‡], Moshe Dessau[§¶], Chiara Salvi[‖], Giovanna Serino[‖], Daniel A. Chamovitz[‡2], and Joel A. Hirsch[§¶3]**

*From the Departments of [‡]Molecular Biology and Ecology of Plants and [¶]Biochemistry and Molecular Biology, [§]Institute for Structural Biology, George S. Wise Faculty of Life Sciences, Tel Aviv University, Ramat Aviv 69978, Israel, [‖]Dipartimento di Biologia e Biotecnologie, Sapienza Università di Roma, Italy, and **The New York Botanical Garden, Bronx, New York 10458*

Background: The COP9 signalosome is a conserved eukaryotic protein complex that regulates protein degradation.
Result: We identified pairwise and combinatorial interactions necessary for the formation of a CSN5-containing subcomplex that binds RBX1.
Conclusion: Three distinct types of protein-protein interactions stabilize the COP9 signalosome.
Significance: This structure enables binding of RBX1 and supports the significance of detected CSN subcomplexes and monomers.

The COP9 signalosome (CSN) is an evolutionarily conserved multi-protein complex that interfaces with the ubiquitin-proteasome pathway and plays critical developmental roles in both animals and plants. Although some subunits are present only in an ~320-kDa complex-dependent form, other subunits are also detected in configurations distinct from the 8-subunit holocomplex. To date, the only known biochemical activity intrinsic to the complex, deneddylation of the Cullin subunits from Cullin-RING ubiquitin ligases, is assigned to CSN5. As an essential step to understanding the structure and assembly of a CSN5-containing subcomplex of the CSN, we reconstituted a CSN4-5-6-7 subcomplex. The core of the subcomplex is based on a stable heterotrimeric association of CSN7, CSN4, and CSN6, requiring coexpression in a bacterial reconstitution system. To this heterotrimer, we could then add CSN5 *in vitro* to reconstitute a quaternary complex. Using biochemical and biophysical methods, we identified pairwise and combinatorial interactions necessary for the formation of the CSN4-5-6-7 subcomplex. The subcomplex is stabilized by three types of interactions: MPN-MPN between CSN5 and CSN6, PCI-PCI between CSN4 and CSN7, and interactions mediated through the CSN6 C terminus with CSN4 and CSN7. CSN8 was also found to interact with the CSN4-6-7 core. These data provide a strong framework for further investigation of the organization and assembly of this pivotal regulatory complex.

The COP9 signalosome (CSN)[4] is a highly conserved eukaryotic protein complex comprising eight subunits named CSN1-CSN8 in order of decreasing molecular mass (1). The complex was originally described as a repressor of light-dependent growth in *Arabidopsis* (2, 3). Subsequent identification and characterization of the CSN from mammalian cells, insects, and yeast demonstrated the complex to be a general modulator of signal transduction (4).

CSN has diverse functions in cellular and developmental processes (4–6). The best studied function is regulation of protein degradation. In this context CSN regulates cullin-RING E3 ligase (CRL) activity by removal of the ubiquitin-like protein, Nedd8, from the cullin subunit of cullin-containing E3 ligases. This deneddylation activity localizes to the JAMM (JAB1/MPN/Mov34)/MPN+) domain of CSN5 (7, 8). However, genomic studies in *Drosophila* suggest that CSN5-dependent deneddylation is only one aspect of CSN function (9). For example, a recent study showed that CSN inhibited CRL4 ubiquitin ligase activity in a non-enzymatic manner (10).

CSN deneddylation activity is dependent on the integrity of the complete CSN complex, composed of six PCI (proteasome, COP9 signalosome, and eukaryotic initiation factor3) domain-containing and two MPN (Mpr1-Pad1-N-terminal) domain-containing subunits. The PCI architecture is built from helical bundle and winged-helix subdomains, where the helical bundle employs HEAT repeats (11, 12). The PCI structural motif is thought to mediate protein-protein interactions (13). While the deneddylation activity resides within CSN5, CSN6, the second MPN domain subunit, lacks enzymatic activity, although it has a role in complex assembly and stability (14).

In mammals (15, 16) and fission yeast (17), CSN5 is necessary for CSN complex integrity. However, several reports of studies

* This work was funded by a grant (145/09) from the Israel Science Foundation (to D. A. C.) and a 2009 Research Grant (Project C26F09JTKN) from Sapienza University (to G. S.).
[S] This article contains supplemental Table 1 and Fig. 1 and 2.
[1] Recipient of a George S. Wise post-doctoral fellowship and support from the Manna Center for Plant Biosciences (Tel Aviv University).
[2] To whom correspondence may be addressed. Tel.: 972-3-6408989; E-mail: dannyc@tauex.tau.ac.il.
[3] To whom correspondence may be addressed: Dept. of Biochemistry and Molecular Biology, George S. Wise Faculty of Life Sciences, Tel Aviv University, Ramat Aviv 69978, Israel. Tel.: 972-3-6406211; E-mail: jhirsch@post.tau.ac.il.

[4] The abbreviations used are: CSN, COP9 signalosome; PCI, proteasome-COP9-eukaryotic initiation factor 3; MPN, MPR1-PAD1-N-terminal domain; HEAT, Huntington, elongation factor 3; HB, helix bundle; WH, winged helix; TEV, tobacco etch virus; SEC, size-exclusion chromatography; MALS, multiangle light scattering; CRL, cullin-RING E3 ligase; Ni^{2+}-NTA, nickel-nitrilotriacetic acid; PR-65/A, TOR.

in *Arabidopsis* and *Drosophila* indicate that loss of CSN5 does not prevent formation of a stable CSN, lacking CSN5 (18, 19). Hence, the exact forms of a "functional" CSN are not always clear. Although some of the eight subunits, such as CSN8, are present only in an ~320-kDa core-"complex-dependent" form, others such as CSN5 and CSN7 are also detected in configurations distinct from the 8-subunit holocomplex. Moreover, several studies have implicated changing equilibria between these different configurations (19–21). This dynamic nature has consequences for experiment interpretation. It is still unclear in many cases which activities and phenotypes of CSN are due to the intact complex and which are due to in the individual subunits or subcomplexes (9).

Further understanding of CSN function should be aided by understanding how this important complex is organized structurally. Indeed, several studies have investigated this question through the use of yeast two-hybrid, mass spectrometry and electron microscopy (8, 22–24). Previously, we elucidated the atomic resolution structure of the CSN7 PCI domain and showed that CSN6 interacted with the CSN7 C-terminal tail (25). Here we document detailed pairwise and combinatorial interactions between CSN subunits as an essential step to understanding the structure and assembly of a CSN5-containing subcomplex of the CSN.

EXPERIMENTAL PROCEDURES

Subcloning and Mutations—All genes are from *Arabidopsis thaliana*. The following constructs were cloned into the pET Duet vector (Novagen) multiple cloning site I: *CSN7* (*CSN7*^{182}, *CSN7*^{187}, *CSN7*^{192}, *CSN7*^{197}, *CSN7*^{mut}), *CSN4*^{full}, using BamHI and NotI by creating an N-terminal His tag for all CSN7 and CSN4 versions. *CSN6* (*CSN6*^{175}, *CSN6*$^{176-312}$ afterward noted as *CSN6*$^{\Delta MPN}$, *CSN6*^{312}) and *CSN7*^{Full} were inserted into multiple cloning site II using NdeI and KpnI. *CSN5b* and *RBX1* were cloned in-frame after a His-tag GST into multiple cloning site I of a pCDF vector. For co-expression of the CSN4-6-7 heterotrimeric complex, *CSN7*^{202} and *CSN4* (*CSN4*^{235}, *CSN4*$^{235-395}$) were subcloned into multiple cloning site I of pCDF vector (Novagen), where the His_6 has been removed. Positive clones were identified by colony PCR and sequenced. Clones of *CSN7*^{202}, *CSN7*^{225} in multiple cloning site I, *CSN6*^{Full} in multiple cloning site II of pET Duet vector, and *CSN1*, *CSN8* constructs in pET28 vector were described previously by Dessau *et al.* (25).

Expression and Purification—All constructs were expressed in *Escherichia coli* T7 Express (New England Biolabs), an enhanced derivative of BL21Plus (Stratagene). Transformed bacteria were inoculated sequentially by increasing volumes of LB growth media at 37 °C. Kanamycin (50 μg/ml) and chloramphenicol (34 μg/ml) were used for CSN1 and CSN8 expression, whereas for co-expression of CSN4-6-7 versions, 25 μg/ml streptomycin, 100 μg/ml ampicillin, and 34 μg/ml chloramphenicol were used, and for CSN7-6 constructs 100 μg/ml ampicillin and 34 μg/ml chloramphenicol were used, whereas for RBX1 and CSN5, 25 μg/ml streptomycin and 34 μg/ml chloramphenicol were used. The cells were grown for 2–3 h in a final volume of 4 liters. The temperature was lowered to 16 °C when A_{600} reached 0.3. Protein expression was induced by 200 μM isopropyl β-D-1-thiogalactopyranoside at A_{600} = 0.5–0.6. Cells were harvested after 12–16 h by centrifugation (9700 × *g*) for 10 min at 4 °C. Cells were suspended at 1:10 w/v ratio in lysis buffer, buffer L (50 mM sodium phosphate, pH 8.0, 300 mM NaCl, 0.1% Triton X-100, 10 mg of lysozyme, 1500 units of DNase, and 5% glycerol). Cells were lysed using a microfluidizer (Microfluidics), and PMSF was added immediately to the lysate (0.2 mM). Cell debris was removed by 1 h of centrifugation (18,000 × *g*) at 4 °C, and the supernatant was loaded onto a pre-equilibrated metal chelate column (Ni^{2+}-NTA, Novagen) (buffer A: 50 mM sodium phosphate, pH 8.0, 300 mM NaCl and 5% glycerol) at flow rate of 1 ml/min. The column was washed with buffer A containing 5 mM imidazole followed by step elution by buffer A supplemented with 50–125 mM imidazole. Fractions containing CSN were pooled and subjected to digestion by TEV protease (26). An additional step of Q-Sepharose column was carried out for CSN4-6^{312}-7^{202} and RBX1 before TEV digestion. CSN4-6^{312}-7^{202} or RBX1 containing fractions were pooled and diluted 5-fold with dilution buffer (10 mM sodium phosphate, 10% glycerol) and loaded onto a pre-equilibrated Q-Sepharose column (25 mM sodium phosphate buffer, 50 mM NaCl). Protein was eluted using a shallow gradient (120 ml) of NaCl (25 mM–1 M). TEV proteolysis was carried out for 12–14 h at 4 °C. Subsequently, the sample was loaded again onto a Ni^{2+}-NTA column with unbound fractions collected and pooled. Imidazole (5 mM) was needed for CSN4-6-7 to elute the digested protein due to nonspecific binding of these proteins to the column. Protein was concentrated to 5 ml using spin concentrators (Amicon Ultra). SEC was then carried out using a pre-equilibrated Superdex 200 HiLoad prep grade column (Amersham Biosciences). Protein was eluted with buffer G (20 mM Tris, pH 7.2, 150 mM NaCl, and 2 mM DTT). Purity of the protein was checked on SDS-PAGE, and fractions were pooled, concentrated into aliquots, and flash-frozen in liquid N_2.

Pulldown Assays—Pulldown assays were performed for truncations of CSN4-6-7, CSN7-6, and mutations of CSN7-6 complexes. 50 ml of culture was grown as described above. Cells were lysed using French press (Aminco) with lysis buffer (50 mM sodium phosphate, pH 8.0, 300 mM NaCl, 0.1% Triton X-100, 10 mg of lysozyme, 1500 units of DNase, and 5% glycerol) with the addition of PMSF (0.2 M). Cell debris was removed by centrifugation for 20 min. The supernatant (1.5 ml) was added to a tube containing 50 μl of Ni^{2+}-NTA beads and kept in end-to-end rotation for 1h at 4 °C. Beads were then washed with Buffer A (buffer A: 50 mM sodium phosphate, pH 8.0, 300 mM NaCl, and 5% glycerol) followed by buffer A containing 5 mM imidazole. Bound proteins were eluted with buffer A containing 125 mM imidazole and checked on SDS-PAGE.

CSN7 Tail Preparation—The CSN7 C terminus tail (residues 170–197) was subcloned into pCDF vector containing maltose-binding protein and TEV recognition site upstream of the MCS I (multiple cloning site I). It was then overexpressed as His_8-maltose-binding protein (MBP) fusion protein in *E. coli* as described above. The protein was purified using standard Ni^{2+}-NTA chromatography, ion-exchange chromatography (Q-Sepharose, Amersham Biosciences) and was then cleaved with TEV

protease followed by Ni^{2+}-NTA chromatography. Fractions containing the CSN7 tail were pooled and concentrated.

CD Spectroscopy—Measurements were performed using a Chirascan CD spectrometer (Applied Photophysics). Cuvette path length used was 0.1 or 1 mm, and sample concentrations were 0.37 mg/ml to 2 mg/ml. Protein buffer contained 10 mM sodium phosphate, pH 8.0, 200 mM NaCl. The purity and monodispersity of samples were checked by SDS-PAGE and analytical size-exclusion chromatography. Each spectrum was averaged from four repeated scans ranging between 180 and 300 nm at a scan rate of 1.25 nm/s. Raw data were corrected by subtracting the contribution of the buffer to the signal. Subtracted data were then smoothed and converted to mean residue molar ellipticity units.

CSN Subunit Interaction Assays—Interacting proteins were incubated in 1:1 molar ratio (100 μM) for 1 h at room temperature. Samples were loaded onto a pre-equilibrated analytical Superdex®200 SEC column (Amersham Biosciences) with buffer G. Individual proteins loading concentrations were 100 μM, and proteins were monitored at 280 nm.

SEC-MALS—SEC-MALS experiments were performed using an analytical SEC column KW404-4F 5 μm 4.6 $\times$ 300-mm (Shodex), equilibrated with 20 mM Tris, pH 7.2, and 150 mM NaCl on an HPLC (Agilent) connected to an 18-angle light-scattering detector (DAWN HELEOS, Wyatt Technology) followed by a differential refractive-index detector (Optilab rEX, Wyatt Technology). 100 μl of the purified protein concentration of 1 mg/ml was loaded onto the analytical column Shodex KW404-4F 5 μm 4.6 $\times$ 300 mm. Data were analyzed with the ASTRA software package (Wyatt Technology).

Analytical Ultracentrifugation—Sedimentation velocity analysis of CSN4-6-7 protein sample were carried out at 40,000 rpm and 20 °C in an XL-I analytical ultracentrifuge (Beckman-Coulter Inc.) with a UV-visible optics detection system using an An60Ti rotor and 12-mm double sector centerpieces. Proteins were equilibrated in 20 mM Tris, 150 mM NaCl, 2 mM dithiothreitol, pH 7.2. The sedimentation velocity runs were done at different protein concentrations ranging from 2 to 4 μM. Sedimentation profiles were registered every min at 280 nm. The sedimentation coefficient distributions were calculated by least-squares boundary modeling of sedimentation velocity data using the $c(s)$ method as implemented in the SEDFIT program. The corresponding standard s-values ($s_{20,w}$) were obtained from the experimental s-values upon correction for density, viscosity, and protein concentration using the SEDNTERP program.

Yeast Two-hybrid Assay—The full-length cDNA clones of *Arabidopsis* CSN6a (27), fused to the activation domain in the pJG vector as well as the full-length cDNA clones of *Arabidopsis* CSN3 (28), CSN4 (29), CSN5a (30), CSN6a (27), CSN7 (31), and CSN7 tail (25) fused to the LexA binding domain in the pEG202 vector have been previously described. To generate the CSN6a deletions clones, the coding region of $CSN6a^{1-136}$, $CSN6a^{1-175}$, $CSN6a^{137-317}$, $CSN6a^{176-317}$ and $CSN6a^{1-303}$ were PCR-amplified and cloned into the pJG vector. Primers are indicated in supplemental Table 1. The LexA fusion constructs were transformed into yeast strain EGY48, whereas activation domain fusion constructs were transformed into yeast strain L40, which contains a β-galactosidase reporter gene. The plate and liquid assays were performed as described previously (32).

Conservation Analysis—Arabidopsis CSN7 amino acid sequence was used as query to search the National Center for Biotechnology Information nonredundant database using BLAST. A manual search of individual sequenced genomes (Ensemble databases) was performed. Eleven CSN7 ortholog sequences that were found and sorted manually were submitted to ClustalW2 on the EMBL-EBI server for multiple sequence alignment. This multiple sequence alignment was then submitted to the Consurf server (33), which uses maximum likelihood method for calculation.

RESULTS

CSN7-6 Interaction—From our previous study (25) it was clear that the CSN7 C-terminal tail is responsible for the interaction with CSN6 and that the interaction was maintained even when amino acids 203–225 were truncated from CSN7. We, therefore, asked what is the minimum length of the CSN7 C-terminal tail required for CSN6 interaction. To answer this question, we constructed additional truncations of CSN7 (Fig. 1*A*). $CSN7^{225}$ and truncated forms $CSN7^{202}$, $CSN7^{197}$, $CSN7^{192}$, $CSN7^{187}$, and $CSN7^{182}$ were co-expressed with CSN6. $CSN7^{225}$ and $CSN7^{202}$ strongly interacted with CSN6, yielding complexes that remained intact even after treatment with 2 M NaCl and 2 M urea (25). $CSN7^{197}$ and $CSN7^{192}$ also interacted with CSN6 but with apparent diminished affinity as manifested in a reduction in the ration of CSN6 to CSN7 (Fig. 1*B*). The interaction between CSN7 and CSN6 was further diminished as the tail was shortened with little interaction between CSN6 and $CSN7^{187}$ or $CSN7^{182}$. The identities of the CSN7 truncations were confirmed by immunoblot (supplemental Fig. 1).

To further identify specific residues involved in the CSN7-6 interaction, we employed scanning alanine mutagenesis of CSN7. Alanine mutations were introduced as triplets from CSN7 residues 168–194 in $CSN7^{197}$. These mutated CSN7 constructs were co-expressed with CSN6. As seen in Fig. 1*C*, mutation of residues 168–173 or residues 183–194 did not abolish the interaction with CSN6. However, no CSN6 was detected when coexpressed with CSN7 containing alanine triplets introduced between residues 174–182, indicating that this region is essential for interaction with CSN6 (Fig. 1*C*).

Further analyses of the amino acid conservation among diverse CSN7 orthologs revealed that within this region tryptophan 177 is completely conserved (Fig. 1*D*). To determine if this residue is directly involved in the CSN7-6 interaction, we introduced point mutations changing this tryptophan to either alanine or aspartate. As seen in Fig. 1*E*, the interaction with CSN6 was strongly reduced in both the point mutations. Almost no CSN6 was recovered when coexpressed with $CSN7^{197}$-W177D, and little CSN6 was recovered when coexpressed with $CSN7^{197}$-W177A. We conclude that tryptophan 177 is a critical residue in the interface of CSN7 and CSN6 (Fig. 1, *D* and *E*).

We then investigated what might be the structure of the CSN7 tail, now clearly established as the binding interface for CSN6. Previous work had shown the full-length tail (170–225)

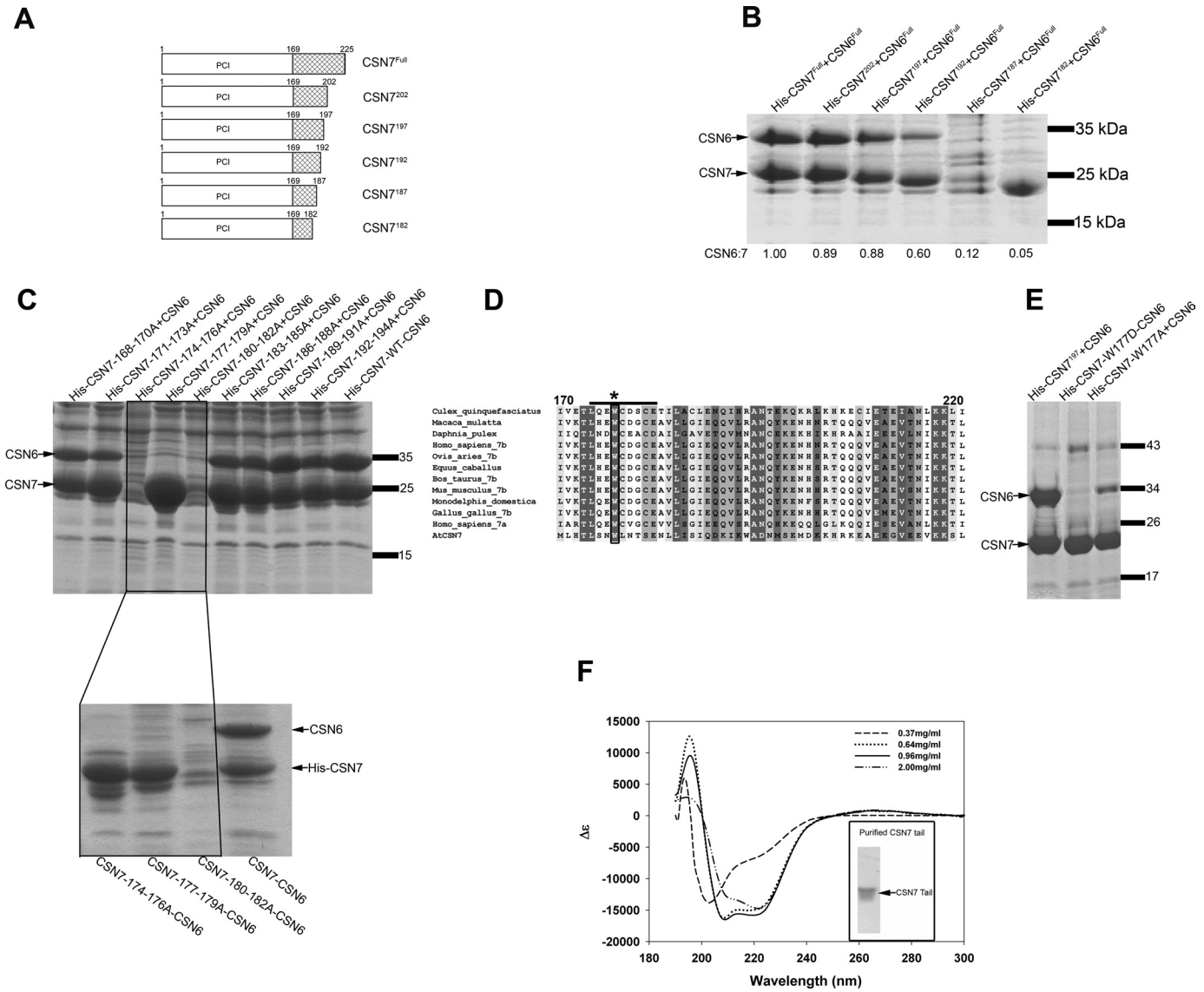

FIGURE 1. **CSN7-6 interaction.** *A*, shown is a schematic depiction of recombinant CSN7 C-terminal tail truncations. These constructs were coexpressed with CSN6. *B*, Coomassie Blue-stained SDS-PAGE shows His-tag pulldown assays of $CSN7^{Full}$ and truncations with CSN6. $CSN7^{Full}$ and $CSN7^{202}$ showed strong interaction with CSN6, where as interaction steeply declined from $CSN7^{197}$. No interaction of CSN6 was observed with the truncations $CSN7^{187}$ and $CSN7^{182}$. Values listed *below each lane* represent the ratio of CSN6 to CSN7 as assessed by densitometry of the displayed gel. *C*, Coomassie Blue stained SDS-PAGE show His-tag pulldown assays of CSN7 C-terminal tail alanine triplet mutations coexpressed with CSN6. $CSN7^{168-173}$ and $CSN7^{183-194}$ showed significant interaction of CSN6, whereas mutations $CSN7^{174-176}$, $CSN7^{177-179}$, and $CSN7^{180-182}$ showed little or no interaction with CSN6. The *lower gel* shows an independent pulldown assay for denoted mutants, confirming that CSN7 triple alanine mutants expressed but did not bind CSN6. *D*, multiple sequence alignment of CSN7 is shown with 11 different orthologs. The region marked $CSN7^{174-182}$ showed no interaction of the CSN6 when mutated to alanine. The residue indicated by an *asterisk* shows Trp-177 conservation, where CSN7-W177A disrupted CSN6 interaction when coexpressed. *E*, Coomassie Blue-stained SDS-PAGE shows His-tag pulldown assays of CSN7-W177 point mutations co-expressed with CSN6. Most of CSN6 was not observed when coexpressed with $CSN7^{197}$-W177D, and little CSN6 was observed when coexpressed with $CSN7^{197}$-W177A. *F*, shown is CD spectroscopic analysis of the $CSN7^{170-197}$ tail at differing concentrations as indicated. The *inset* shows a SDS-PAGE of the purified $CSN7^{170-197}$ tail.

to be unstructured (25). Having now more precisely defined the CSN6 binding site, we purified the CSN7 truncated C-tail, residues 170–197, and measured the CD spectrum in the concentration range of 0.3 to 2 mg/ml. Disordered structure of the truncated tail was observed at 0.3 mg/ml, whereas increasing concentrations indicated increasing fractions of helical secondary structure (Fig. 1*F*). Such behavior is consistent with intrinsically disordered protein that upon association with protein undergoes a structured transition, facilitating binding with its target, here expected to be CSN6 (34).

CSN4-6-7 Heterotrimeric Complex—CSN4 is a PCI protein that interacts with both CSN7 and CSN6 (22–24). Having specifically defined the region of CSN7 necessary for the interaction with CSN6, we next asked how this heterodimer interacts with CSN4. When expressed alone in *E. coli*, CSN4 expression is limited. However, when co-expressed with CSN6 and CSN7, expression was robust, and a stable, soluble heterotrimeric complex of CSN4-6-7 could be detected.

However, we could not purify this complex to homogeneity due to apparent partial degradation of CSN6. Indeed, SDS-PAGE analyses revealed that ~1.6 kDa is truncated from CSN6 (supplemental Fig. 2). Subsequent N-terminal sequencing revealed an intact N terminus of CSN6 in this preparation, suggesting that CSN6 is digested from the C terminus. Further

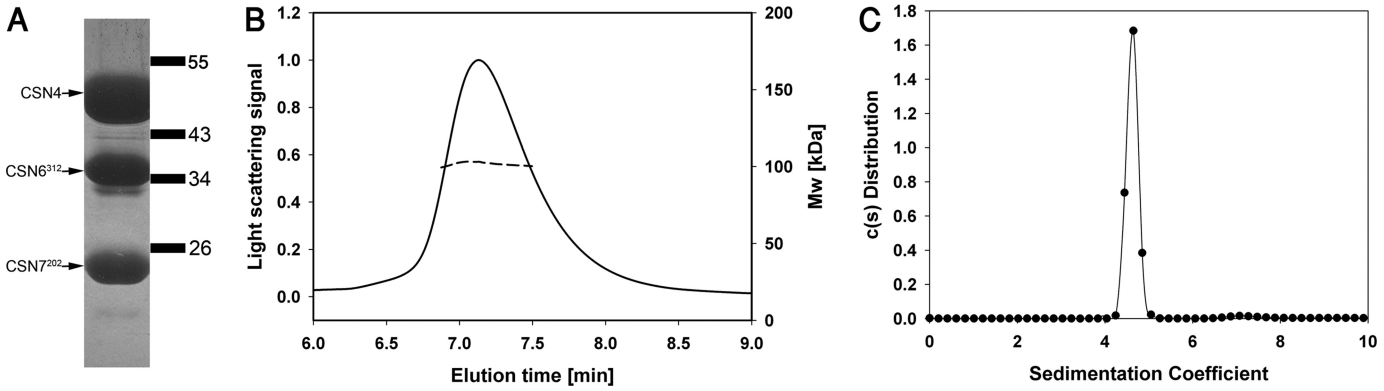

FIGURE 2. **CSN4-6-7 heterotrimeric complex.** *A*, Coomassie Blue-stained SDS-PAGE showing the purified ternary complex of CSN4-6^{312}-7^{202} coexpressed in *E. coli*. *B*, SEC-MALS of purified CSN4-6^{312}-7^{202} ternary complex shows the mass of ~100 kDa, indicating the complex is intact. *C*, sedimentation analysis shows CSN4-6^{312}-7^{202} complex is monodisperse, having a sedimentation coefficient of 4.88 *s* and a frictional ratio (f/f_0) of 1.58 at 2 μM concentration. The sedimentation was performed at 40,000 rpm at 20 °C.

deletion analysis showed that removal of only five amino acids from the C terminus of CSN6, *i.e.* $CSN6^{312}$, resulted in a degradation-resistant protein when co-expressed with CSN4 and $CSN7^{202}$, yielding a heterotrimeric complex subunit with an apparent stoichiometric ratio of 1:1:1 (Fig. 2*A*).

Multiangle light scattering results confirm that the complex is intact with a molecular mass of 101 kDa (Fig. 2*B*), as expected for a 1:1:1 complex. Furthermore, sedimentation velocity studies indicate that the complex is homogeneous and monodisperse (Fig. 2*C*) with a sedimentation coefficient of 4.88 *s* and a frictional ratio (f/f_0) of 1.58 at 2 μM concentration. These values are stable for at least a 2-fold concentration range.

CSN4 Interacts with Both CSN6 and CSN7—Further experiments were carried out to determine whether CSN4 directly interacts with CSN6 or CSN7. A His-tagged version of CSN4 was co-expressed in *E. coli* with either CSN7 or CSN6 separately, and Ni^{2+}-NTA beads were used to pull down CSN4 from the protein lysate. As seen in Fig. 3*A*, CSN6 clearly co-purified with His-CSN4. The CSN4 interaction with CSN7 was not clearly observed by SDS-PAGE; however, immunoblot analysis using α-CSN7 or α-CSN6 antibodies confirmed that both proteins were present in the pulldown with CSN4 (Fig. 3*B*). The results indicate that CSN4 interacts with both CSN6 and CSN7, although the interaction with CSN6 may be of higher affinity.

Based on earlier protein-interaction studies (22–24), we hypothesized that the interaction between CSN4 and CSN7 in the heterotrimeric CSN4-6-7 complex is mediated through PCI-PCI domain interactions. This hypothesis was tested by co-expressing CSN7 and CSN6 together with a CSN4 construct lacking the PCI domain. Constructs of CSN4 were designed to separate CSN4 into PCI and ΔPCI forms (Fig. 3*C*). $CSN4^{\Delta PCI}$ did not facilitate the formation of the heterotrimeric complex of $CSN4^{\Delta PCI}$-6–7. On the other hand, $CSN4^{PCI}$ interacts with CSN7 and CSN6 to form the CSN4-6-7 complex, indicating that the PCI domain of CSN4 acts as the scaffold for CSN4-6-7 interaction (Fig. 3*D*).

Previously, based on our crystallographic study, we identified surface residues on different faces of the CSN7 HB and WH subdomains and mutated these residues, mapping interaction interfaces for CSN8 (25). To further map CSN4 and CSN6 interactions with CSN7, these CSN7 mutants, namely D12A, E44A, and H71A located in the HB subdomain and K144A, E153A located in the WH subdomain were tested in copurification assays (Fig. 3*E*). When $CSN7^{202}$, mutated for these various residues, was coexpressed with CSN4 and CSN6, pulldown experiments indicated that the CSN4-6^{312}-7^{202} heterotrimeric complex was disrupted when either single or double CSN7 mutants containing the E44A and/or H71A mutations were employed, whereas the $CSN7^{202}$-CSN6 complex formation was not affected (Fig. 3*F*) in the presence of these mutations. We, therefore, conclude that CSN4 interacts with the CSN7 HB subdomain.

MPN Domain of CSN6 Is Not Required for CSN4-6-7 Complex Integrity—Having dissected the interactions of the two PCI subunits in this complex, we next turned to understand the contribution of CSN6. CSN6 contains an N-terminal MPN domain and a newly identified S6CD domain in the carboxyl half of the protein (35). We first employed the yeast two-hybrid assay to determine which domains of CSN6 contribute to its interaction with CSN7. As expected, CSN6 interacted in this assay with CSN5, CSN7, and the C-terminal tail of CSN7 but not with the PCI-domain of CSN7 (Fig. 4*A*). Although the MPN domain alone of CSN6 interacted with CSN5, it did not interact with CSN7 or with the CSN7 C-tail. On the other hand, the S6CD-containing C-terminal half of CSN6 did interact with CSN7.

To further confirm these interactions *in vitro*, two constructs of CSN6 were constructed, $CSN6^{MPN}$, which contains residues 1–175 including the MPN domain, and $CSN6^{\Delta MPN}$, encoding residues 176–312 (Fig. 4*B*). These constructs of CSN6 were co-expressed with CSN7 alone or with CSN7 and CSN4 together. Co-purification assays reveal a robust interaction between $CSN6^{\Delta MPN}$ and CSN7 and with CSN7 and CSN4 (Fig. 4*C*). However, no interaction was observed with the construct $CSN6^{MPN}$, indicating that the MPN domain is dispensable for the formation of the heterotrimeric complex.

Interaction of CSN4-6-7 Complex with Other Subunits—The SEC assay is a convenient method to check subunit interactions (25). Various interaction studies had indicated that CSN7 interacts with both CSN8 and CSN1 (22, 23, 25), whereas a mass spectrometry-based model of the entire complex did not sup-

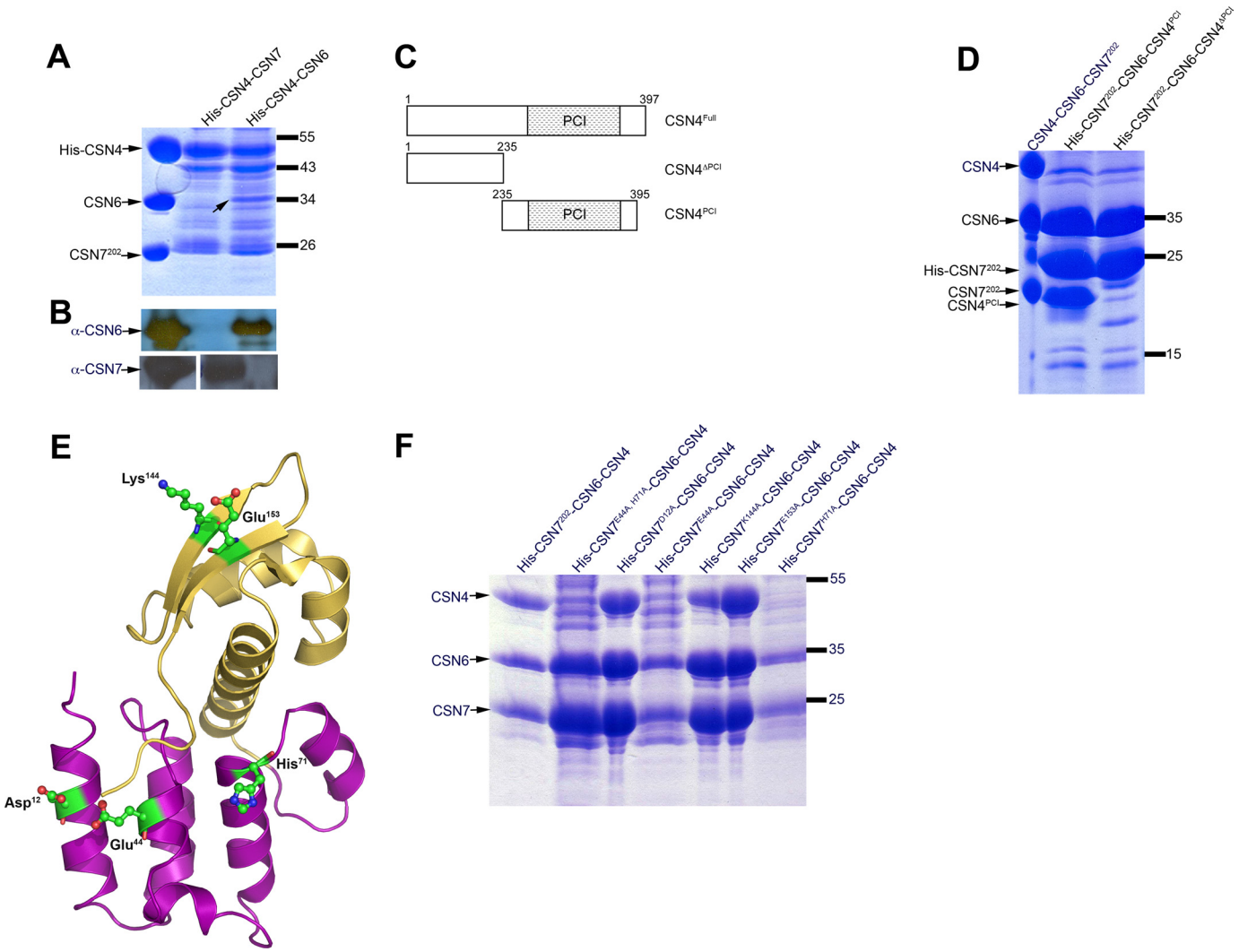

FIGURE 3. **CSN4 interactions with CSN6 and CSN7.** *A*, Coomassie Blue stained SDS-PAGE shows His-tag pulldown assays of CSN4-7and CSN4-6 coexpressed in *E. coli*, where CSN4 was His-tagged. The *arrow* indicates the CSN6 band. *B*, shown is Western blot analysis of gel in *panel A*, confirming the interaction of CSN4-6 and CSN4-7 as probed with α-CSN6 and α-CSN7 antibodies as indicated. *C*, shown is a schematic depiction of truncations of CSN4 coexpressed with CSN6 and CSN7. *D*, shown is Coomassie Blue-stained SDS-PAGE showing the interaction of the heterotrimeric complex, CSN4-6-7^{202} (*left lane*). The *middle lane* shows $CSN4^{PCI}$, containing the PCI domain (residues 235–395), in complex with CSN6 and $CSN7^{202}$. Deletion of the CSN4 PCI domain abrogates the interaction (*right lane*). *E*, shown is a *ribbon/sticks* representation of CSN7 point mutants. The HB and WH subdomains are colored *magenta* and *yellow*, respectively. *F*, Coomassie Blue-stained SDS-PAGE shows CSN7 point mutations coexpressed with CSN4 and $CSN6^{312}$. Mutations on E44A and H71A disrupted the CSN4-6^{312}-7^{202} complex.

port such an interaction (24). To determine if CSN8 or CSN1 can interact with the CSN4-6^{312}-7^{202} heterotrimeric complex to form a ternary complex, CSN4-6^{312}-7^{202} was incubated with either CSN8 or CSN1 and then analyzed by SEC. As seen in Fig. 5, *A* and *B*, CSN4-6^{312}-7^{202} interacts with CSN8, forming a heterotetrameric complex, CSN4-6^{312}-7^{202}-8. However, the CSN4-6^{312}-7^{202} complex did not show interaction with CSN1 (Fig. 5, *C* and *D*).

Yeast two-hybrid, mass spectrometry and cryo-EM studies indicated a stable tetrameric complex of CSN4-5-6-7 (8, 22–24). The SEC assay was used to check the interaction of CSN5 with CSN4-6^{312}-7^{202}. A CSN4-5-6^{312}-7^{202} complex was observed when analyzed by SEC (Fig. 6, *A* and *B*), whereas no direct interaction of CSN5 was observed with $CSN7^{197}$ alone (Fig. 6, *C* and *D*).

To map the interface responsible for CSN5 or CSN8 binding to the CSN4-6-7 complex, we purified a CSN4-$6^{\Delta MPN}$-7^{202} complex to homogeneity, and its interaction was checked by SEC-MALS with CSN5 and CSN8. CSN5 did not bind to a CSN4-$6^{\Delta MPN}$-7^{202} complex, indicating that the MPN domain of CSN6 is required for CSN4-5-6-7 complex formation (Fig. 6*E*). In contrast, CSN8 interacts with a CSN4-$6^{\Delta MPN}$-7^{202} complex, as observed by the increase of molecular mass in SEC-MALS, forming a CSN4-$6^{\Delta MPN}$-7^{202}-8 heterotetrameric complex (Fig. 6*F*). We reconstituted a heteropentameric complex comprising CSN4-5-6-7-8 by incubation of purified CSN4-6-7 with purified CSN5 and CSN8. This material was then run on a SEC column, and the SDS-PAGE of the elution peak shows all subunits that co-elute (Fig. 6*G*).

RBX1 Interacts with the CSN4-5-6-7 Subcomplex—Both catalytic and non-catalytic activities of the CSN *vis à vis* protein degradation require binding to CRLs (10, 36, 37). Protein interaction studies indicated that this interaction is partially mediated through the binding of CSN6 to RBX1 (38). We, therefore, asked whether this interaction is maintained in the CSN4-5-6-7 subcomplex of the CSN.

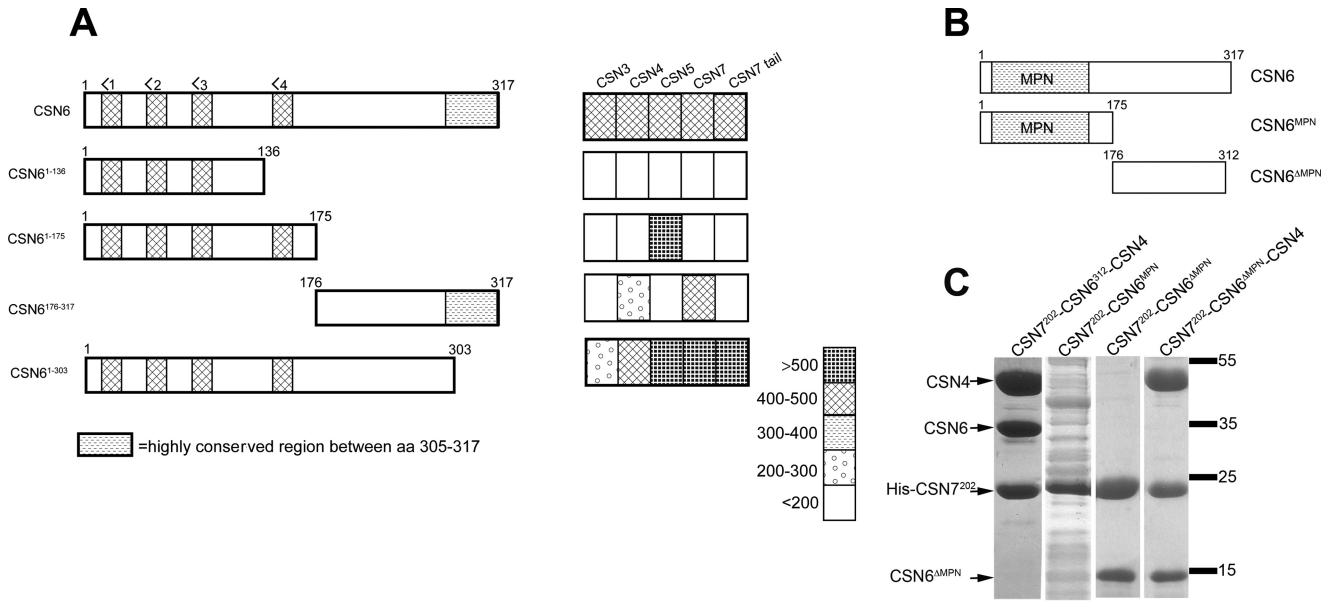

FIGURE 4. **The MPN domain is not required for assembly of the CSN7-6 and CSN4-6-7 complexes.** *A*, yeast two-hybrid analysis shows the interaction of CSN subunits with CSN6 truncations. The *left panel* illustrates the CSN6 deletions used in the prey constructs. *Boxes* designated with *>1*, *>2*, *>3*, and *>4* indicate the four α helices, whereas the box at the C terminus indicates a conserved region of CSN6 spanning amino acids 305–317. The *right panel* shows the corresponding β-galactosidase activities of the interaction with CSN subunits 3, 4, 5, and 7 and the CSN7 C-terminal tail (CSN7$^{170-225}$). The *legend at the bottom right corner* indicates the relative β-galactosidase activities values in Miller units. *B*, shown is a schematic depiction of CSN6 truncations coexpressed with CSN7^{202} and with both CSN7^{202} and CSN4. *C*, Coomassie Blue-stained SDS-PAGE show heterotrimeric CSN4-6-7 complex (*left lane*), removal of residues 176–317 from CSN6 (denoted CSN6^{MPN}) abrogates interaction with CSN7 (*second lane*), purified CSN7^{202}-CSN6$^{\Delta MPN}$ (*third lane*), and CSN4-CSN6$^{\Delta MPN}$-CSN7^{202} (*right lane*) complexes.

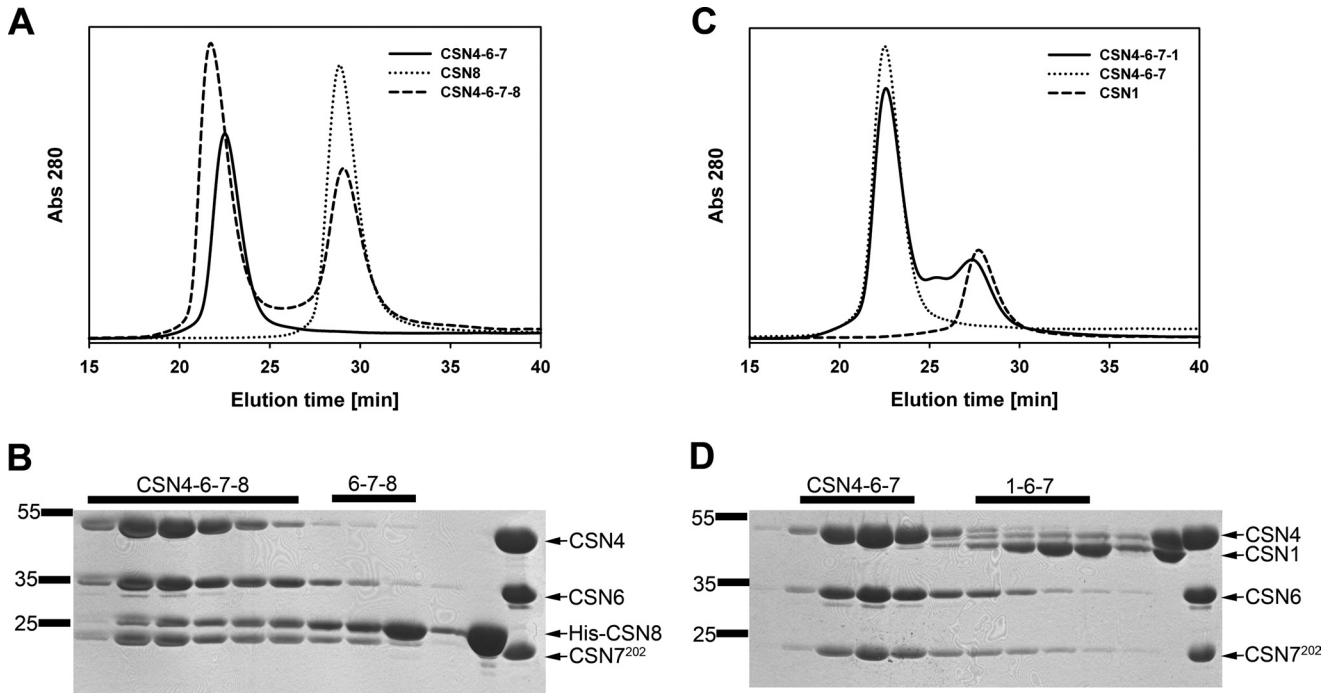

FIGURE 5. **Assembly of CSN subcomplexes involving CSN8 or CSN1.** *A*, a SEC elution profile shows the peak shift, indicating the CSN4-6^{312}-7^{202}-8 tetrameric complex formation. *B*, Coomassie Blue-stained SDS-PAGE of SEC fractions from *panel A* show interaction of CSN4-6^{312}-7^{202}-8 complex. *C*, SEC elution profile indicates that CSN1 does not stably interact with the CSN4-6^{312}-7^{202} complex. *D*, shown is a Coomassie Blue-stained SDS-PAGE of SEC fractions from *panel C*. CSN1 does not interact with the CSN4-6^{312}-7^{202} complex.

The SEC assay was used to check the interaction of RBX1 with CSN4-5-6^{312}-7^{202}. RBX1 from *Arabidopsis* was expressed in *E. coli*, purified to near homogeneity, and incubated with the CSN4-5-6^{312}-7^{202} tetrameric complex, isolated as in the previous section. As seen in Fig. 7, RBX1 alone elutes in low molecular weight fractions. After incubation with the CSN subcomplex, RBX1 co-eluted with the CSN subunits. We conclude that the CSN4-5-6-7 subcomplex retains a functional organization, configured for potential binding to a CRL.

DISCUSSION

We have identified robust pairwise and combinatorial interactions necessary for the formation of a CSN5-containing subcomplex of the CSN and showed that this subcomplex is sufficient for mediating interactions with the CRL subunit RBX1. The core of the subcomplex is based on a stable heterotrimeric association of CSN7, CSN4, and CSN6. Notably, Sharon *et al.*, (24) observed that recombinant CSN complexes can be dissociated into two principal stable subcomplexes, one containing CSN7, CSN6, and CSN4.These results are also consistent with earlier protein-protein interaction studies (22, 23, 25, 39). To reconstitute such a complex in *E. coli*, coexpression of both

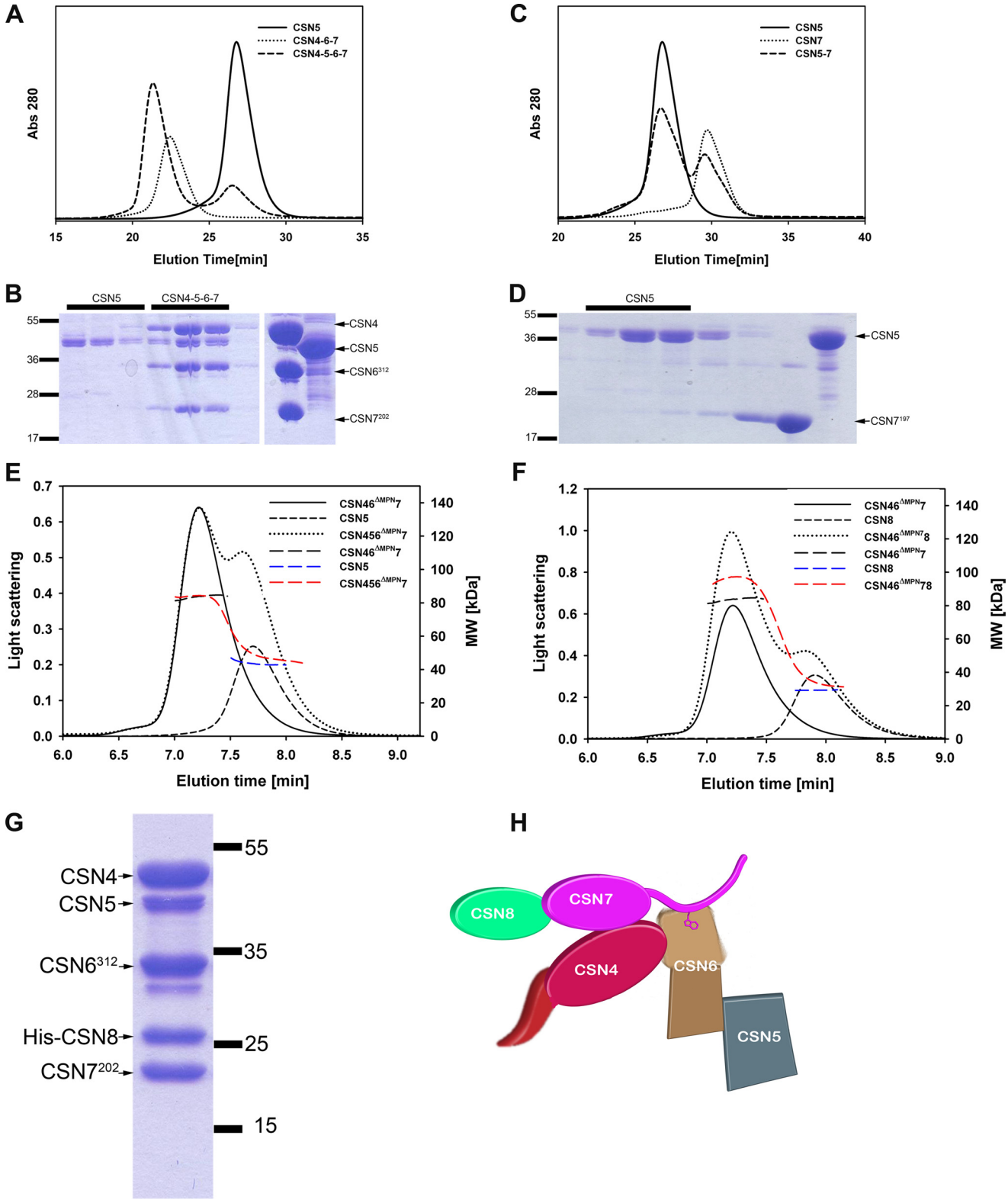

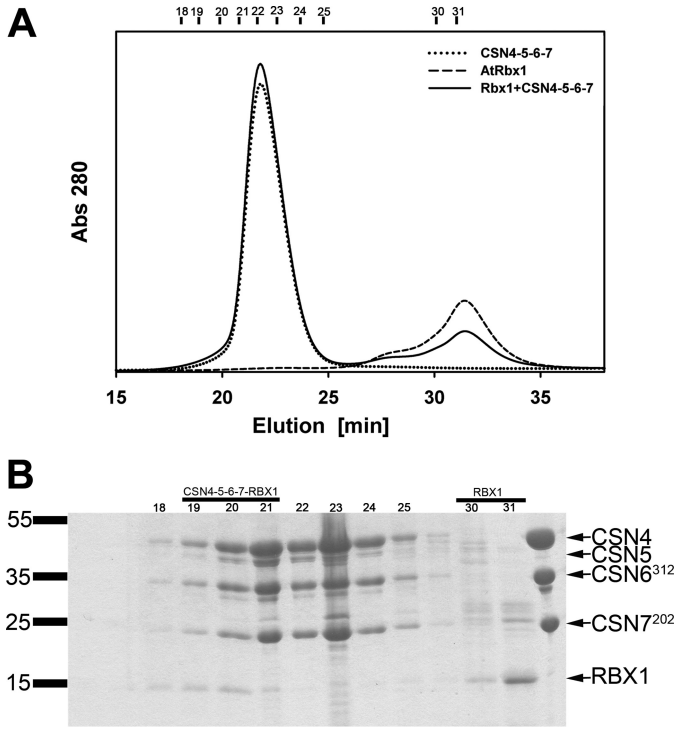

FIGURE 7. **Assembly of a CSN4-5-6-7 subcomplex with RBX1.** *A*, a SEC elution profile of RBX1 interaction with CSN4-5-6^{312}-7^{202} shows co-elution of RBX1 with the CSN subcomplex (fractions 19–21). The elution of RBX1 alone is found at a greater elution volume (fractions 30–31). The three SEC experiments (RBX1 alone, CSN subcomplex alone, RBX1-CSN subcomplex mixture) are denoted. The amount of CSN subcomplex used was identical. *B*, shown is Coomassie Blue-stained SDS-PAGE of fractions from the RBX1-CSN subcomplex mixture SEC run, in *panel A*.

CSN4 and CSN6 with CSN7 was required, as only CSN7 appears stable alone, and the expression or either CSN4 or CSN6 alone was severely limited. To this heterotrimer, we could then add CSN5 *in vitro* to reconstitute a quaternary complex.

From the different deletion constructs analyzed here, we propose a model whereby this subcomplex is organized via distinct interaction surfaces (Fig. 6*G*). Our model shows that CSN6 is a core protein in the subcomplex, interacting with CSN4, CSN5, and CSN7. The non-MPN part of the CSN6 is in association with CSN4 and CSN7, whereas the CSN6 MPN domain is responsible for the interaction with CSN5. This central positioning of CSN6 fits earlier genetic studies in *Arabidopsis*, which showed that complete loss of CSN6 results in loss of the entire CSN complex (14).

Previously, we reported that CSN7 comprises an N-terminal PCI domain and a C-terminal tail extending from the residues 170–225 and that this tail was essential for CSN6 stability *in vitro* and CSN function *in vivo* (25). Here, we further narrowed the CSN6 binding site to the CSN7 tail proximal to the PCI domain. Although $CSN7^{202}$ was found sufficient to interact with CSN6 at a 1:1 ratio, the apparent stability of this interaction declined as the CSN7 tail was truncated, and little or no interaction was observed with CSN6 with truncation of $CSN7^{187}$or $CSN7^{182}$. Scanning alanine mutagenesis on $CSN7^{197}$ revealed that the region between amino acids 174 and 182 is important for interaction with CSN6. Within this region, Trp-177 was identified as essential for the CSN7-CSN6 interaction. The importance of this residue in mediating the CSN7-CSN6 interaction is further underscored by its evolutionary conservation. Although the overall level of amino acid conservation in the C-terminal tail of CSN7 is not high, Trp-177 is completely conserved in all orthologs.

The interaction between CSN7 and CSN4 is dependent on PCI-PCI interactions. Furthermore, the CSN4 PCI domain is also required for association with the non-PCI protein, CSN6. These interactions then conceivably leave the C-terminal half of CSN4 (amino acids 235–395) available for interaction with extra-complex proteins. In this vein, this end of CSN4 would be similar to the distal regions of the CSN7 tail, which bind a variety of proteins such as RNR2 and PCIP1 (40), and the non-PCI region of CSN1, which has transcriptional transactivation activity (41). The C-terminal half of CSN6 is required for its interaction with both CSN4 and CSN7, leaving its MPN domain available for interaction with CSN5. How this fits with a recent report where the MPN domain is not essential for CSN5-mediated deneddylation is not clear (35). Our preparation of a heterotrimer of CSN4, CSN6, and CSN7 may best fit with earlier findings that both *Arabidopsis* and *Drosophila* CSN5 appeared to be nonessential for complex formation (18, 19), in contrast to another report which showed that CSN5 does appear to be essential for complex formation (14).

The CSN4-5-6-7 subcomplex is stabilized by three types of interactions: MPN-MPN, PCI-PCI, and interactions mediated through the CSN6 C terminus. How does our working model compare with current ones? Although the structural model proposed by Sharon *et al.* (24) with two subcomplexes *i.e.* CSN1-2-3-8 and CSN4-5-6-7, has provided a framework for subsequent studies, it did not predict many of the binary interactions previously reported for CSN subunits, such as between CSN7 and CSN8. Here, we show that at least one subunit of the CSN1-2-3-8 subcomplex, namely CSN8, can stably associate with a CSN4-6-7 heterotrimer. Interestingly, although the CSN7-CSN1 interaction has been shown by several different assays (25), we were unable to detect an interaction between CSN1 and the CSN4-6^{312}-7^{202} heterotrimer even though a

FIGURE 6. **Assembly of CSN subcomplexes; implications of domain deletions.** *A*, shown is a SEC elution profile of CSN5 interaction with CSN4-6^{312}-7^{202} that shows a shift in peak indicating 4-5-6^{312}-7^{202} heterotetrameric complex formation. *B*, Coomassie Blue-stained SDS-PAGE of SEC fractions from *panel A* show the interaction of CSN5 with CSN4-6^{312}-7^{202}. The *extreme right lanes* show relevant CSN protein standards. *C*, the SEC elution profile of CSN5 interaction with $CSN7^{197}$ is shown. No shift in the elution peak was observed. CSN5 was incubated with $CSN7^{197}$ for 1 h at room temperature and analyzed. *D*, Coomassie Blue-stained SDS-PAGE of SEC fractions from *panel C* shows no interaction between CSN5 and $CSN7^{197}$. The *extreme right lanes* show relevant CSN protein standards. *E*, SEC-MALS shows CSN5 does not interact with CSN4-$6^{\Delta MPN}$-7^{202} complex. CSN5 was incubated with CSN4-$6^{\Delta MPN}$-7^{202} complex for 1 h at room temperature and analyzed. *F*, SEC-MALS shows interaction of CSN8 with CSN4-$6^{\Delta MPN}$-7^{202} complex. Molecular mass was increased after interaction, which is ~100 kDa. CSN8 was incubated with CSN4-$6^{\Delta MPN}$-7^{202} complex for 1 h at room temperature and analyzed. *G*, shown is a Coomassie Blue-stained SDS-PAGE of a reconstituted, purified CSN4-5-6-7-8 complex. *H*, shown is a working model of a CSN subcomplex, summarized by schematic depiction of the CSN4-6-7 core subcomplex and its interactions with other CSN subunits. *Ovals* indicate PCI domains, whereas *rectangles* denote MPN domains. The extension extending from CSN4 depicts the HEAT/TPR repeat structure N-terminal to its PCI domain. The CSN7 tail is drawn explicitly with the conserved Trp to which CSN6 binds.

CSN4-6-1-8 was detected (24), perhaps implying that a number of subcomplex permutations are biochemically possible, if not physiologically relevant. Alternatively, assembly order may be critical to formation of the native CSN.

Our results also fit well with the CSN model proposed by Enchev *et al.* (8) based on cryo-EM single particle analysis. These workers observed three connections between what they assign to be the small and large "segments," where segments correspond to CSN4-5-6-7 and CSN1-2-3-8 subcomplexes, respectively. This finding suggests that the two subcomplexes then will have more than one interface, in contrast to the single CSN1–6 interface postulated by Sharon *et al.* (24). Our data regarding CSN7-8 interactions in the context of the CSN4-6-7 core could then represent one of the additional interfaces. Moreover, other data, reviewed by Pick *et al.* (42), as well as more recent EM findings on the 19 S proteasome lid (43, 44) demonstrate that MPN-MPN domain-containing subunits interact directly in each of the three PCI-MPN complexes.

Many publications have reported CSN subunits as monomers or as part of smaller complexes than the full eight-subunit CSN. However, it is not clear whether these forms have biological significance or are experimental artifacts occurring during biochemical isolation. Many of these reports concern CSN5, which would also fit with our findings presented here (20, 45), as it appears as if the core subcomplex is CSN4-6-7. For example, a cytoplasmic complex containing CSN4-5-6-7b-8 was also reported in mammalian cells (46).

In light of recent publications claiming a noncatalytic structural role for the CSN in regulation of CRLs (10, 37), the binding of RBX1 by the subcomplexes studied here opens the possibilities that different conformations of CSN subunits may interact with CRLs to regulate their activity. Further investigation is required to test the physiological relevance of such subcomplexes.

Acknowledgments—We thank Yehezkel Sasson and Anna Vitlin for assistance with light-scattering and analytical centrifugation and Orna Chomsky-Hecht and Lior Almagor for advice on subcloning, mutagenesis, and protein purification.

REFERENCES

1. Deng, X. W., Dubiel, W., Wei, N., Hofmann, K., and Mundt, K. (2000) Unified nomenclature for the COP9 signalosome and its subunits. An essential regulator of development. *Trends Genet.* **16,** 289
2. Chamovitz, D. A., Wei, N., Osterlund, M. T., von Arnim, A. G., Staub, J. M., Matsui, M., and Deng, X. W. (1996) The COP9 complex, a novel multisubunit nuclear regulator involved in light control of a plant developmental switch. *Cell* **86,** 115–121
3. Wei, N., Chamovitz, D. A., and Deng, X. W. (1994) *Arabidopsis* COP9 is a component of a novel signaling complex mediating light control of development. *Cell* **78,** 117–124
4. Wei, N., Serino, G., and Deng, X. W. (2008) The COP9 signalosome. More than a protease. *Trends Biochem. Sci.* **33,** 592–600
5. Harari-Steinberg, O., and Chamovitz, D. A. (2004) The COP9 signalosome. Mediating between kinase signaling and protein degradation. *Curr. Protein Pept. Sci.* **5,** 185–189
6. Cope, G. A., and Deshaies, R. J. (2003) COP9 signalosome. A multifunctional regulator of SCF and other cullin-based ubiquitin ligases. *Cell* **114,** 663–671
7. Cope, G. A., Suh, G. S., Aravind, L., Schwarz, S. E., Zipursky, S. L., Koonin, E. V., and Deshaies, R. J. (2002) Role of predicted metalloprotease motif of Jab1/Csn5 in cleavage of Nedd8 from Cul1. *Science* **298,** 608–611
8. Enchev, R. I., Schreiber, A., Beuron, F., and Morris, E. P. (2010) Structural insights into the COP9 signalosome and its common architecture with the 26 S proteasome lid and eIF3. *Structure* **18,** 518–527
9. Oron, E., Tuller, T., Li, L., Rozovsky, N., Yekutieli, D., Rencus-Lazar, S., Segal, D., Chor, B., Edgar, B. A., and Chamovitz, D. A. (2007) Genomic analysis of COP9 signalosome function in *Drosophila melanogaster* reveals a role in temporal regulation of gene expression. *Mol. Syst. Biol.* **3,** 108
10. Fischer, E. S., Scrima, A., Böhm, K., Matsumoto, S., Lingaraju, G. M., Faty, M., Yasuda, T., Cavadini, S., Wakasugi, M., Hanaoka, F., Iwai, S., Gut, H., Sugasawa, K., and Thomä, N. H. (2011) The molecular basis of CRL4DDB2/CSA ubiquitin ligase architecture, targeting, and activation. *Cell* **147,** 1024–1039
11. Scheel, H., and Hofmann, K. (2005) Prediction of a common structural scaffold for proteasome lid, COP9-signalosome and eIF3 complexes. *BMC Bioinformatics* **6,** 71
12. Hofmann, K., and Bucher, P. (1998) The PCI domain. A common theme in three multiprotein complexes. *Trends Biochem. Sci.* **23,** 204–205
13. Wei, N., and Deng, X. W. (2003) The COP9 signalosome. *Annu. Rev. Cell Dev. Biol.* **19,** 261–286
14. Gusmaroli, G., Figueroa, P., Serino, G., and Deng, X. W. (2007) Role of the MPN subunits in COP9 signalosome assembly and activity, and their regulatory interaction with *Arabidopsis* Cullin3-based E3 ligases. *Plant Cell* **19,** 564–581
15. Tomoda, K., Yoneda-Kato, N., Fukumoto, A., Yamanaka, S., and Kato, J. Y. (2004) Multiple functions of Jab1 are required for early embryonic development and growth potential in mice. *J. Biol. Chem.* **279,** 43013–43018
16. Denti, S., Fernandez-Sanchez, M. E., Rogge, L., and Bianchi, E. (2006) The COP9 signalosome regulates Skp2 levels and proliferation of human cells. *J. Biol. Chem.* **281,** 32188–32196
17. Mundt, K. E., Liu, C., and Carr, A. M. (2002) Deletion mutants in COP9/signalosome subunits in fission yeast *Schizosaccharomyces pombe* display distinct phenotypes. *Mol. Biol. Cell* **13,** 493–502
18. Dohmann, E. M., Kuhnle, C., and Schwechheimer, C. (2005) Loss of the Constitutive Photomorphogenic9 signalosome subunit 5 is sufficient to cause the cop/det/fus mutant phenotype in *Arabidopsis*. *Plant Cell* **17,** 1967–1978
19. Oron, E., Mannervik, M., Rencus, S., Harari-Steinberg, O., Neuman-Silberberg, S., Segal, D., and Chamovitz, D. A. (2002) COP9 signalosome subunits 4 and 5 regulate multiple pleiotropic pathways in *Drosophila melanogaster*. *Development* **129,** 4399–4409
20. Fukumoto, A., Tomoda, K., Kubota, M., Kato, J. Y., and Yoneda-Kato, N. (2005) Small Jab1-containing subcomplex is regulated in an anchorage- and cell cycle-dependent manner, which is abrogated by ras transformation. *FEBS Lett.* **579,** 1047–1054
21. Tsuge, T., Matsui, M., and Wei, N. (2001) The subunit 1 of the COP9 signalosome suppresses gene expression through its N-terminal domain and incorporates into the complex through the PCI domain. *J. Mol. Biol.* **305,** 1–9
22. Fu, H., Reis, N., Lee, Y., Glickman, M. H., and Vierstra, R. D. (2001) Subunit interaction maps for the regulatory particle of the 26 S proteasome and the COP9 signalosome. *EMBO J.* **20,** 7096–7107
23. Serino, G., Su, H., Peng, Z., Tsuge, T., Wei, N., Gu, H., and Deng, X. W. (2003) Characterization of the last subunit of the *Arabidopsis* COP9 signalosome. Implications for the overall structure and origin of the complex. *Plant Cell* **15,** 719–731
24. Sharon, M., Mao, H., Boeri Erba, E., Stephens, E., Zheng, N., and Robinson, C. V. (2009) Symmetrical modularity of the COP9 signalosome complex suggests its multifunctionality. *Structure* **17,** 31–40
25. Dessau, M., Halimi, Y., Erez, T., Chomsky-Hecht, O., Chamovitz, D. A., and Hirsch, J. A. (2008) The *Arabidopsis* COP9 signalosome subunit 7 is a model PCI domain protein with subdomains involved in COP9 signalosome assembly. *Plant Cell* **20,** 2815–2834
26. Opatowsky, Y., Chomsky-Hecht, O., Kang, M. G., Campbell, K. P., and Hirsch, J. A. (2003) The voltage-dependent calcium channel β subunit contains two stable interacting domains. *J. Biol. Chem.* **278,** 52323–52332

27. Peng, Z., Serino, G., and Deng, X. W. (2001) Molecular characterization of subunit 6 of the COP9 signalosome and its role in multifaceted developmental processes in *Arabidopsis*. *Plant Cell* **13,** 2393–2407
28. Peng, Z., Serino, G., and Deng, X. W. (2001) A role of *Arabidopsis* COP9 signalosome in multifaceted developmental processes revealed by the characterization of its subunit 3. *Development* **128,** 4277–4288
29. Serino, G., Tsuge, T., Kwok, S., Matsui, M., Wei, N., and Deng, X. W. (1999) *Arabidopsis* cop8 and fus4 mutations define the same gene that encodes subunit 4 of the COP9 signalosome. *Plant Cell* **11,** 1967–1980
30. Kwok, S. F., Solano, R., Tsuge, T., Chamovitz, D. A., Ecker, J. R., Matsui, M., and Deng, X. W. (1998) *Arabidopsis* homologs of a c-Jun coactivator are present both in monomeric form and in the COP9 complex, and their abundance is differentially affected by the pleiotropic cop/det/fus mutations. *Plant Cell* **10,** 1779–1790
31. Karniol, B., Malec, P., and Chamovitz, D. A. (1999) *Arabidopsis* FUSCA5 encodes a novel phosphoprotein that is a component of the COP9 complex. *Plant Cell* **11,** 839–848
32. Golemis, E. A., and Khazak, V. (1997) Alternative yeast two-hybrid systems. The interaction trap and interaction mating. *Methods Mol. Biol.* **63,** 197–218
33. Ashkenazy, H., Erez, E., Martz, E., Pupko, T., and Ben-Tal, N. (2010) ConSurf 2010. Calculating evolutionary conservation in sequence and structure of proteins and nucleic acids. *Nucleic Acids Res.* **38,** W529–W533
34. Turoverov, K. K., Kuznetsova, I. M., and Uversky, V. N. (2010) The protein kingdom extended. Ordered and intrinsically disordered proteins, their folding, supramolecular complex formation, and aggregation. *Prog. Biophys. Mol. Biol.* **102,** 73–84
35. Pick, E., Golan, A., Zimbler, J. Z., Guo, L., Sharaby, Y., Tsuge, T., Hofmann, K., and Wei, N. (2012) The minimal deneddylase core of the COP9 signalosome excludes the Csn6 MPN(−) domain. *Plos One* **7,** e43980
36. Lyapina, S., Cope, G., Shevchenko, A., Serino, G., Tsuge, T., Zhou, C., Wolf, D. A., Wei, N., Shevchenko, A., and Deshaies, R. J. (2001) Promotion of NEDD-CUL1 conjugate cleavage by COP9 signalosome. *Science* **292,** 1382–1385
37. Emberley, E. D., Mosadeghi, R., and Deshaies, R. J. (2012) Deconjugation of Nedd8 from Cul1 is directly regulated by Skp1-F-box and substrate, and the COP9 signalosome inhibits deneddylated SCF by a noncatalytic mechanism. *J. Biol. Chem.* **287,** 29679–29689
38. Schwechheimer, C., Serino, G., Callis, J., Crosby, W. L., Lyapina, S., Deshaies, R. J., Gray, W. M., Estelle, M., and Deng, X. W. (2001) Interactions of the COP9 signalosome with the E3 ubiquitin ligase SCFTIRI in mediating auxin response. *Science* **292,** 1379–1382
39. Kapelari, B., Bech-Otschir, D., Hegerl, R., Schade, R., Dumdey, R., and Dubiel, W. (2000) Electron microscopy and subunit-subunit interaction studies reveal a first architecture of COP9 signalosome. *J. Mol. Biol.* **300,** 1169–1178
40. Halimi, Y., Dessau, M., Pollak, S., Ast, T., Erez, T., Livnat-Levanon, N., Karniol, B., Hirsch, J. A., and Chamovitz, D. A. (2011) COP9 signalosome subunit 7 from *Arabidopsis* interacts with and regulates the small subunit of ribonucleotide reductase (RNR2). *Plant Mol. Biol.* **77,** 77–89
41. Menon, S., Chi, H., Zhang, H., Deng, X. W., Flavell, R. A., and Wei, N. (2007) COP9 signalosome subunit 8 is essential for peripheral T cell homeostasis and antigen receptor-induced entry into the cell cycle from quiescence. *Nat. Immunol.* **8,** 1236–1245
42. Pick, E., Hofmann, K., and Glickman, M. H. (2009) PCI complexes. Beyond the proteasome, CSN, and eIF3 Troika. *Mol. Cell* **35,** 260–264
43. da Fonseca, P. C., He, J., and Morris, E. P. (2012) Molecular model of the human 26S proteasome. *Mol. Cell* **46,** 54–66
44. Lander, G. C., Estrin, E., Matyskiela, M. E., Bashore, C., Nogales, E., and Martin, A. (2012) Complete subunit architecture of the proteasome regulatory particle. *Nature* **482,** 186–191
45. Tomoda, K., Kato, J. Y., Tatsumi, E., Takahashi, T., Matsuo, Y., and Yoneda-Kato, N. (2005) The Jab1/COP9 signalosome subcomplex is a downstream mediator of Bcr-Abl kinase activity and facilitates cell-cycle progression. *Blood* **105,** 775–783
46. Tomoda, K., Kubota, Y., Arata, Y., Mori, S., Maeda, M., Tanaka, T., Yoshida, M., Yoneda-Kato, N., and Kato, J. Y. (2002) The cytoplasmic shuttling and subsequent degradation of p27Kip1 mediated by Jab1/CSN5 and the COP9 signalosome complex. *J. Biol. Chem.* **277,** 2302–2310